Features of the Arctic Stratosphere during IPY

E. Farahani, SPARC IPO, University of Toronto, Canada (elham@atmosp.physics.utoronto.ca)
N. McFarlane, SPARC IPO, University of Toronto, Canada (Norm.McFarlane@ec.gc.ca)
R.L. Batchelor, University of Toronto, Canada (rbatchelor@atmosp.physics.utoronto.ca)
R.L. Collins, Geophysical Institute and Department of Atmospheric Sciences, University of Alaska Fairbanks, USA (rlc@gi.alaska.edu)
V.L. Harvey, University of Colorado, USA, (lynn.harvey@lasp.colorado.edu)
N.J. Livesey, Jet Propulsion Laboratory, California Institute of Technology, USA (livesey@mls.jpl.nasa.gov)
G.L. Manney, Jet Propulsion Laboratory, California Institute of Technology, USA (Gloria.L.Manney@jpl.nasa.gov)
M.L. Santee, Jet Propulsion Laboratory, California Institute of Technology, USA (Michelle.L.Santee@jpl.nasa.gov)
K. Strong, University of Toronto, Canada (strong@atmosp.physics.utoronto.ca)
K.A. Walker, University of Toronto, Canada (kwalker@atmosp.physics.utoronto.ca)

Introduction

The International Polar Year (IPY) has provided the opportunity and the means to intensify and coordinate ground-based measurements from stations across the Arctic. The combination of ground-based measurements, complimented by satellite observations, affords a unique observational framework for studying atmospheric processes in the Arctic during the IPY period. Many of the ground-based stations are affiliated with the Network for the Detection of Atmospheric Composition Change (NDACC: **http://www.ndacc.org/**). NDACC stations typically have a suite of instruments, including lidars (for measuring ozone, water vapour, aerosol, and temperature profiles), microwave radiometers (ozone, water vapour, and ClO profiles), UV-visible spectrometers (ozone, NO_2, OClO and BrO columns), Fourier transform infrared (FTIR) spectrometers (columns of many species), Dobson and Brewer spectrophotometers (ozone columns), sondes (ozone and aerosol profiles), and UV spectroradiometers (UV radiation at the ground). Fourier transform infrared spectrometers provide a particularly valuable tool for characterising the chemical composition of the Arctic atmosphere, as they can measure both stratospheric and tropospheric species, such as ozone, HCl, HF, NO, NO_2, $ClONO_2$, HNO_3, N_2O, CO, CH_4, C_2H_6, and HCN. More information concerning the FTIR spectrometers within the NDACC can be found at **http://www.acd.ucar.edu/irwg**.

During IPY, satellite observations, particularly those focused on the polar winter middle atmosphere, provided details on the meteorology and insight into chemical and dynamical processes. The Aura Microwave Limb Sounder (MLS) (Waters *et al*., 2006) and the Atmospheric Chemistry Experiment - Fourier Transform Spectrometer (ACE-FTS) (Bernath *et al*., 2005) are two valuable sensors that provide daily measurements from which temperature and trace gas data have been extracted since 2004. These data sets cover the upper troposphere through the mesosphere.

This unique combination of ground-based and satellite observations are now being used to study and elucidate many dynamical and chemical features of the Arctic stratosphere and mesosphere. The purpose of this article is to provide a broad overview of the observations and highlight some of these features during the IPY period.

Dynamical features of the Stratospheric and Mesospheric Circulation during IPY

A number of recent studies of the planetary scale circulation during the IPY period have utilised temperature and geopotential height data determined from satellite observations. In addition, lidar measurements of density and temperature fluctuations enable identification of higher frequency, smaller-scale features in the upper stratosphere and mesosphere that are associated with gravity-wave propagation. In combination, these satellite and ground-based measurements have revealed a range of dynamical features and processes that have occurred in the Arctic stratosphere and mesosphere during the IPY period. Many of these features are manifestations of well known, *albeit* irregularly occurring, phenomena (such as stratospheric warmings) that have been studied in the past. However, as is noted repeatedly in this summary article, the coincidence of observations from satellite and ground-based systems during the IPY period has enabled identification and study of many of these features in greater detail than may have been possible in the past, or may be possible in the future if some of the observing systems do not continue to operate. This section will provide an overview of significant dynamical features of the Arctic winter stratosphere and mesosphere that have been identified in the IPY period.

Large-Scale Structure

The three winters 2006-2007, 2007-2008 and 2008-2009 represent a wide range of conditions in the highly variable Arctic winter stratosphere, though only 2008-2009 exhibits an extreme of Arctic variability (*e.g*. Manney *et al*., 2008a). **Figure 1** (colour plate I) shows zonal-mean zonal winds in the middle and upper stratosphere in each year. Both 2006-2007 and 2007-2008 were cold, relatively undisturbed winters (strong westerlies). A brief major stratospheric sudden warming[1] (SSW)

[1]An SSW is considered major when the zonal mean wind and temperature gradient pole-ward of 60ºN change sign at 10hPa.

occurred in late February in both 2007 and 2008. After the SSW in February 2007, the vortex reformed and reestablished westerlies persisted through early April, resulting in an unusually late final warming. In 2008, the first major SSW was followed very closely by a "major final" warming (that is, a major warming leading directly into the final warming without recovery of westerlies in between), resulting in an early vortex breakup before mid-March. In January 2009, the strongest, most prolonged SSW on record occurred (*e.g*. Manney *et al*., in press); after this event, 10hPa winds returned to westerlies as a weak vortex was reestablished, and the final warming was late (as is typical after early major SSWs, *e.g*. Manney *et al*., 2005, 2008b), in early May. The overall evolution of the vortex prior to the SSWs at 10hPa is similar in both 2007 and 2008. However in the upper stratosphere (*e.g*. 1hPa), there were numerous brief wind reversals in 2008 prior to the major SSW. The prolonged major SSW in 2009 resulted in an ~10-day wind reversal in the upper stratosphere, after which very strong westerlies reappeared, indicating reformation of an unusually strong upper stratospheric vortex.

Figure 2 (colour plate I) shows the evolution of high latitude temperatures during the three winters. The polar winter stratopause (temperature maximum) is typically near 50 km, and shows considerable variability in temperature and position. Similar to the behaviour during the prolonged major SSW in 2006 (*e.g* Siskind *et al*., 2007; Manney *et al*., 2008a, b), the stratopause dropped dramatically, then broke down during the 2009 SSW; reformation of the stratopause at a very high altitude after the SSW was accompanied by enhanced descent and reestablishment of an unusually strong upper stratospheric vortex (Manney *et al*., in press), similar to 2006 (*e.g*. Siskind *et al*., 2007; Manney *et al*., 2008a, b); reformation of a strong vortex was seen in the development of strong westerlies at 1 hPa as shown in Figure 1. The brief major SSWs in February 2007 and 2008 had only a small effect on the stratopause location and temperatures, and, consistent with the occurrence later in the season, the vortex did not strongly reform (see Figure 1). In the lower stratosphere, temperatures in December and early January were lower in 2007-2008 and 2008-2009 than in 2006-2007; however, low temperatures persisted longest in 2007, until late February, as opposed to mid-February in 2008 and (because of the major SSW) late January in 2009.

Figure 3 (colour plate II) shows maps of scaled potential vorticity (sPV, see Manney *et al*., 1994 for details of scaling) in the lower (490K), middle (850K), and upper (1700K) stratosphere, and in the lower mesosphere or near the stratopause (2500K) from the GEOS-5 assimilated meteorological analyses. The date shown in each year is at the beginning of the major SSW, approximately the time when the 10 hPa zonal-mean winds reversed to easterly. SSWs are classified as vortex displacement or vortex split events (*e.g*. Charlton and Polvani, 2007); 2007 and 2008 provide examples of the first type (displacement) and 2009 of the second (split). SSWs typically develop from the top down (*e.g*. Andrews *et al*., 1987), and, consistent with this, the upper stratospheric and lower mesospheric vortex had already broken down by the date shown, and the lower stratospheric vortex, while strongly distorted, was still intact. In 2007 and 2008, the lower stratospheric vortex did not subsequently break down, as the influence of those brief major SSWs was not that deep; in 2009 the lower stratospheric vortex broke down completely in early February and never reformed (Manney *et al*., in press).

Figure 4 (colour plate II) shows ACE-FTS measurements of long-lived trace gases in the Arctic polar vortex during the IPY winters. The increase in CH_4 and N_2O and decrease in CO surrounding the late-December to January gap in vortex coverage is an artifact of the ACE-FTS sampling moving from vortex core (lower CH_4 and N_2O, higher CO) to vortex edge beforehand, and from edge to core afterwards (*e.g*. Manney *et al*., 2007, 2009). Other variations are consistent with the patterns seen in MLS measurements (*e.g*. Manney *et al*. (in press) show MLS vortex averaged CO and N_2O for 2009; Manney *et al*., 2009 show MLS and ACE vortex averages for the 2005-2006 winter). In December and early January, CO (and to some extent CH_4) show the early winter descent of mesospheric air into the polar vortex in each year, but the variations in the extent of the signature highlights the large interannual variability in descent (closely linked to temperature variability) and vortex isolation in the upper stratosphere. In 2009, that signature of confined descent is abruptly terminated in mid-January, at the start of the major SSW; as the upper stratospheric vortex reformed, a signature of strong confined descent was seen once again. Manney *et al*., (in press) show these features in MLS data, and very similar behaviour was seen in ACE-FTS and MLS data during the strong January 2006 SSW (Manney *et al*., 2009). A similar, but weaker, signature is seen during the brief February 2007 and February 2008 major SSWs; the stronger signature in 2008 results partly from mesospheric air having descended further into the stratosphere vortex before the SSW in that year, but also is consistent with the somewhat stronger SSW in 2008 than 2007 (*e.g*. Figure 1).

Harvey *et al*. (2002) have developed a methodology for depicting aspects of the three-dimensional structure and evolution of the polar vortex. **Figure 5** (colour plate III) shows snapshots for days corresponding to warming onsets during the year 2007, 2008, and 2009. Full animations may be viewed on the SPARC-IPY website (**http://www.atmosp.physics.utoronto.ca/SPARC-IPY/**).

Lidar Observations of Temperature in the Stratosphere and Mesosphere in the Arctic Winter

A network of five Rayleigh lidars has conducted soundings of the stratosphere and mesosphere during the IPY winters (*i.e*. 2007-2008, 2008-2009). The location of the lidars is shown in **Figure 6**. These lidars provide high-resolution measurements of temperature in the stratosphere and mesosphere, and have previously contributed to validation of the measurements from the Atmospheric Chemistry Experiment (ACE) satellite (Sica *et al*., 2008). **Figure 7** shows temperature profiles measured by the lidars in February 2009. The temperature profiles represent an average temperature measured over several hours at nighttime. The measurements at these high latitude sites highlight the longitudinal asymmetries in the circulation of the Arctic stratosphere and mesosphere (*e.g*. Thurairajah *et al*., 2009). Thurairajah *et al*. (2009) presents and compares a variety of temperature measurements from satellites, ground-based instruments, and *in situ* instruments in the Arctic with comparisons to the SPARC atlas. For 2009, measurements at Kühlungsborn, Germany (54°N, 12°E) show a temperature

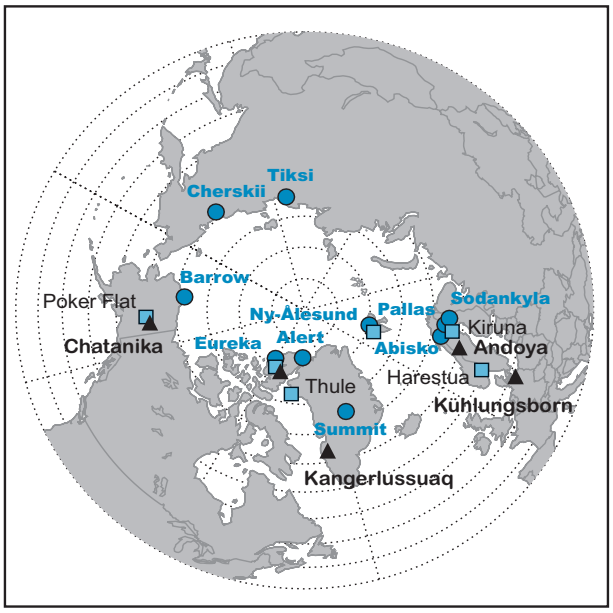

Figure 6. The locations of the IASOA observatories (cyan circles) and the six NDACC stations north of 60° that have FTIR spectrometers (blue squares). Eureka and Ny Ålesund are in both networks. The black triangles show the locations of a network of five Rayleigh lidar sites making ongoing measurements of the middle atmosphere during the IPY. Adapted from IASOA (http://www.iasoa.org).

profile similar to the climatology in the stratosphere and lower mesosphere, with a temperature enhancement in the upper mesosphere. The high latitude measurements at Chatanika, USA (65°N, 147°W), Andoya, Norway (69°N, 16°W), and Eureka (PEARL), Canada (80°N, 86°W) all show an upper stratosphere and lower mesosphere significantly colder than climatology. All four sites show a temperature enhancement in the upper mesosphere. At the highest latitude sites of Andoya and Eureka, the temperature profiles show the structure of an "elevated stratopause" with a cold stratosphere in 2004 and 2006 (Hauchecorne *et al*., 2007; Siskind *et al*., 2007) consistent with MLS measurements shown in Figure 2.

The presence of a separated winter stratopause in the polar region is currently understood as a manifestation of the dynamical coupling between the mesosphere and the lower atmosphere, particularly in association with wave driving that accompanies gravity-wave saturation (Hitchmann *et al*., 1989). It is often a pronounced wintertime feature in both the Antarctic and the Arctic. Its presence and role in the evolution of the stratosphere in the Arctic in recent winters has been noted in observational and modelling studies (Siskind *et al*., 2007, Hoffmann *et al*., 2007) where its strong coupling to stratospheric warmings has also been examined (Manney *et al*., 2008b). This coupling is also consistent with the role of gravity-wave driving in determining the structure of the polar winter stratopause. In this region, the gravity wave driving is most likely associated with upward-propagating orographically excited gravity waves. During stratospheric warmings, strong weakening or reversal of the zonal westerly winds in the stratosphere effectively filters these waves in the lower stratosphere. Removing the gravity wave forcing from the diabatic circulation in the mesosphere typically inhibits relaxation of the atmosphere in that region toward a radiative equilibrium state. Restoration of westerly winds, in association with stratospheric cooling following the warming, again permits upward propagation of these gravity-waves with the associated wave saturation and wave driving in the mesosphere.

Although this interpretation of the role of gravity wave driving is consistent with the observed behaviour of the polar winter stratopause, corroborating direct observations of the gravity wave activity and its variation in the upper stratosphere and mesosphere during and following stratospheric warming events are not usually reported. However, Rayleigh lidar observations yield measurements of the atmospheric density profile at 30-min resolution. The density measurements can be combined with the nightly temperature to yield measurements of the potential energy of the gravity-wave fluctuations (*e.g*. Wilson *et al*., 1991). **Figure 8** shows the relative density fluctuations measured by the Rayleigh lidar at Chatanika on February 11, 2008. **Figure 9** shows the gravity wave potential energies measured at three of the lidar sites in early 2008 (*i.e*. Kühlungsborn, Chatanika and Kangerlussuaq, Greenland). The gravity wave energies at Chatanika are generally lower than Kühlungsborn and Kangerlussuaq. Figure 9 also shows the magnitude of the stratospheric winds at these three sites in early 2008. The low wave energies at Chatanika are consistent with the weaker winds. Ray tracing studies have shown that the weaker winds associated with the Aleutian anticyclone result in blocking of

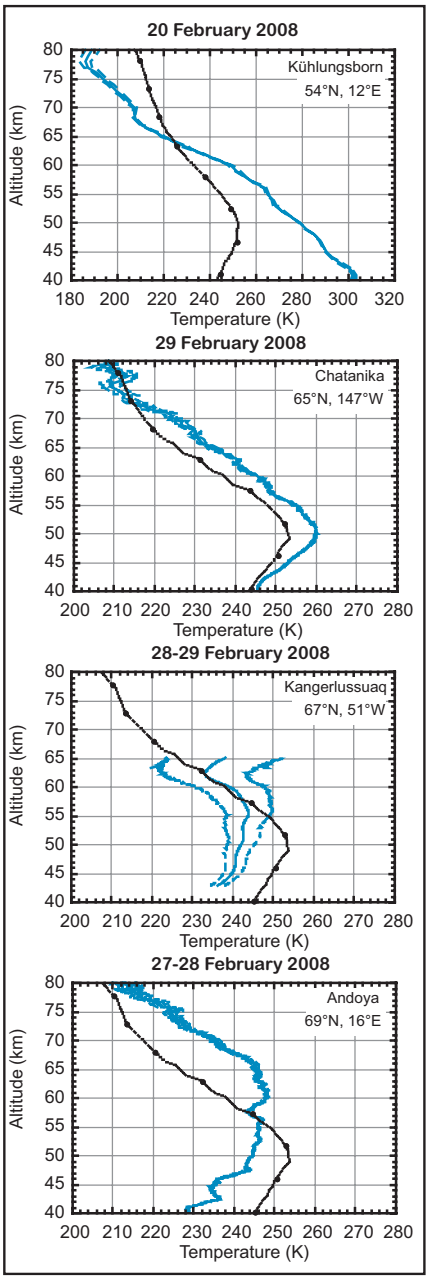

Figure 7. Rayleigh lidar temperatures (blue solid) plotted as a function of altitude from four northern hemisphere sites in February 2008. The uncertainty in the lidar measurements is also plotted (blue dashed). The SPARC reference atlas temperatures are plotted for comparison (black dashed with dot).

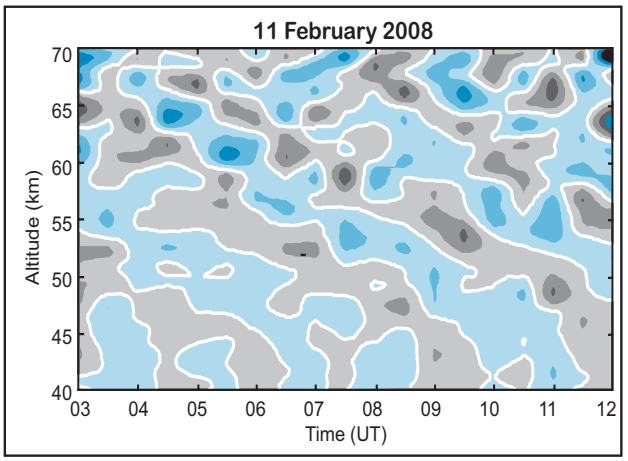

Figure 8. Relative density fluctuations as a function of time and altitude measured by Rayleigh lidar at Chatanika, Alaska (65°N, 147°W). The white contour marks the 0% fluctuation, 0–1% (light grey), 1–2% (medium grey), >2% (dark grey), 0–-1% (light blue), -1–-2% (medium blue) <-2% (dark blue). Data represents fluctuations with observed periods 1 h – 4 h, and vertical wavelengths 2 – 30 km.

upwardly propagating orographic gravity waves (*e.g.* Dunkerton and Butchart, 1984). Studies of the gravity wave activity in early 2009, to see how gravity wave activity is affected by the major change in the Arctic stratospheric circulation in February 2009, are in progress. Direct observations of the gravity wave activity will allow assessment of the role of gravity waves in the evolution of the Arctic winter stratopause as exemplified by formation of the "elevated stratopause" described by Siskind *et al.* (2007).

Stratospheric Chemistry during IPY

In the Arctic stratosphere, average ozone column amounts show high interannual variability, with low ozone values in late winter and spring during cold winters when the Arctic polar vortex breakup occurs late in spring, and high ozone values during warm winters with a disturbed vortex (WMO, 2007). Both dynamically-driven processes, such as those discussed here and chemically-driven processes such as heterogeneous chemistry and halogen activation contribute to variability in Arctic ozone. However, the extent to which each of these basic winter processes affect Arctic ozone varies strongly from year to year. Extreme ozone depletion has been observed when vortex temperatures were low enough to sustain polar stratospheric clouds over a period of few days, while little or no ozone loss was observed during warm winters with a disturbed vortex (WMO, 2007). The low temperatures of an extremely cold Arctic polar vortex may sustain polar stratospheric clouds and/or prolong their existence (*e.g.* Singleton *et al.*, 2007) leading to substantial chlorine activation (Santee *et al.*, 2008 and references therein). To investigate the influence of chemical processes on the stratospheric ozone distribution in the Arctic atmosphere, and to monitor the ozone recovery in the future, it is crucial to have continuous high-quality measurements of ozone and its related constituents in the stratosphere (WMO, 2007). While satellite-borne instruments provide near global coverage of the stratosphere with high spatial resolution, ground-based observations complement them with high temporal resolution that can be used to provide insight into local processes.

Satellite Measurements Across the Arctic

Aura MLS provides observations of many species important to polar process studies, including HNO_3, HCl, ClO, H_2O, and ozone, as well as long-lived tracers such as N_2O, that are important in assessing the relative effects of dynamical and chemical processes. MLS data have been used in numerous studies of polar processing, including studies of large ozone losses in the 2004-2005 winter (*e.g.* Manney *et al.*, 2006, Singleton *et al.*, 2007), examination of the effects of a vortex intrusion on polar processing (Schoeberl *et al.*, 2006), and a comprehensive study of chlorine partitioning in several Arctic and Antarctic winters (Santee *et al.*, 2008). **Figures 10** and **11** (colour plate III and IV) provide an overview of MLS observations of polar processing during the three IPY winters.

Figure 10 shows equivalent latitude[2] (EqL) time series of MLS HCl, ClO and ozone in the lower stratosphere (490K, ~50hPa, ~18km) during the past three winters. Black overlaid contours show the regions where temperatures - averaged around EqL contours - were below the approximate threshold for polar stratospheric cloud (PSC) formation; localised regions of temperatures low enough for PSC formation were present both before and after the periods indicated here (when the cold area was large enough to appear in this average). As noted in the previous section, low temperatures persisted longest in 2007, but were lower during the cold periods in 2008 and 2009. In each year, decreasing HCl and increasing ClO heralds activation of chlorine through reactions on PSCs. The patterns of both depressed HCl and enhanced ClO de-

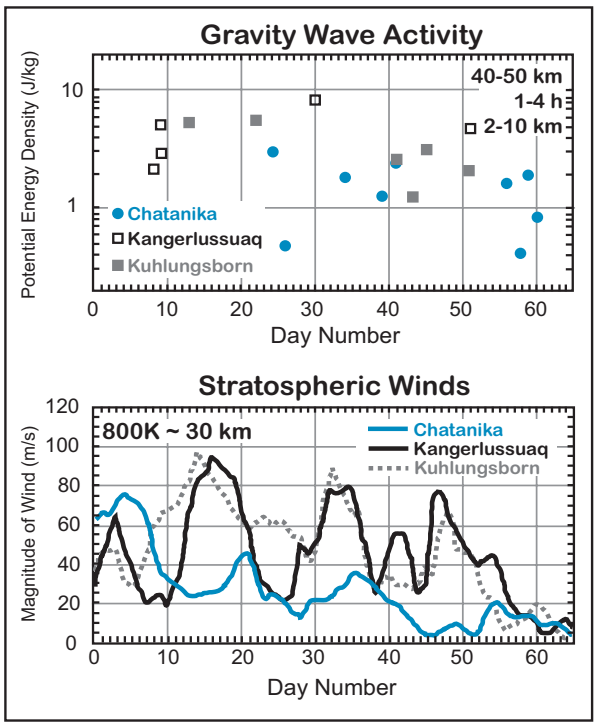

Figure 9. (Upper) Potential energy of gravity waves measured in early 2008 at Kühlungsborn (54°N, 12°E), Chatanika (65°N, 147°W) and Kangerlussuaq (67°N, 51°W) as a function of day number (1 = January 1). (Lower) Magnitude of 800K winds from (UK) Meteorological Office as a function of day number at corresponding locations.

[2]The latitude that would enclose the same area between it and the pole as a given PV contour, commonly used as a vortex-centered coordinate.

pend not only on the temperatures, but also on the location of the cold region with respect to the vortex and strong winds, which determines how extensively and where PSC-processed air is transported within the vortex (*e.g*. Manney *et al*., 2003). In addition, ClO enhancement occurs primarily in sunlit regions. Thus, the differences in patterns of chlorine activation depend on many aspects of the circulation. Substantial chlorine activation began in mid-late December in each year, with activated chlorine filling most of the vortex by late January in 2007 and 2008, and by mid-January in 2009. Similar timing of activation was seen in earlier winters observed by MLS (Santee *et al*., 2008).

The earlier extensive activation in 2009 is consistent with a more distorted, active vortex, of which larger portions experience sunlight, and throughout which processed air is transported more extensively. Similar early activation was seen in 2005-2006 in the active, distorted vortex prior to the January major SSW in that year (Santee *et al*., 2008). Chlorine activation was more complete in 2008 than in 2007, consistent with lower temperatures in 2008. Activation persisted until late March 2007, mid-March 2008, and was curtailed by mid-February 2009 as a result of the major SSW. In each year, vortex ozone begins to decline by late January to early February. Since transport processes (primarily descent in the vortex) tend to increase ozone, the decrease is an indication of chemical loss. In 2009, the decrease halts after a few weeks, as the vortex breaks up during the major SSW, so chemical loss was not extensive. Ozone continued to decrease through early March in 2007 and 2008, over a broader region and somewhat more quickly in 2008 than in 2007.

Figure 11 shows the vertical extent of observed polar processing in the three winters as vortex averages (within an sPV contour) of HNO_3, HCl, ClO and ozone in the lower through middle stratosphere. In the lower stratosphere, the averages after late February 2009 are not useful since the lower stratospheric vortex had broken up. Decreases in HNO_3 indicate sequestration in PSCs; the decreases do not appear very dramatic in these vortex averages because the region of sequestration (low temperatures) typically does not fill the vortex. The largest HNO_3 decreases in early 2008 indicate most extensive PSC activity in that year. HCl and ClO show the longest-lasting, most intense, and deepest vertical extent of chlorine activation in early 2008, with long-lasting activation also in 2007, and early deactivation in 2009 after the major SSW. The upward tilt of ozone contours indicates decreasing vortex ozone; this began in late January in 2007 and 2009, and in early February in 2008. In 2008, lower ozone values appear somewhat sooner at higher levels (near/above 20 km), consistent with chlorine activation extending to higher levels.

While the observed differences in ozone in the three IPY years appear consistent with differences in temperatures and chlorine activation, transport processes play such an important role in the distribution of Arctic ozone that separating dynamical and chemical effects, and thus quantifying chemical ozone loss, requires much more detailed analysis. Methods for doing so typically involve using either transport models or long-lived trace gas measurements to quantify transport (*e.g*. WMO, 2007). State-of-the-art data assimilation systems (such as GEOS-5, ECMWF and others in the SPARC-IPY database) provide high-quality winds for transport calculations; Aura MLS measurements of N_2O provide a long-lived tracer that is useful for assessing transport processes.

ACE-FTS on SCISAT provides measurements that complement those obtained by Aura MLS. Profiles of over 30 different species are retrieved from the ACE solar occultation spectra. These include species such as ozone, HCl, $ClONO_2$, HNO_3, and NO_2 that are valuable for studies of polar ozone chemistry and the long-lived species N_2O, CH_4 and HF that are needed to understand the transport of the air masses of interest. Prior to IPY, the ACE-FTS measurements from winter 2004-2005 were used to investigate partitioning of inorganic chlorine between the two reservoir species HCl and $ClONO_2$ (Dufour *et al*., 2006), and to study denitrification in the Arctic vortex using correlations with long-lived tracers (Jin *et al*., 2006). Enhancements in NO_x in the Arctic vortex, due to strong downward transport of NO produced by energetic particle precipitation, were studied by Randall *et al*. (2006) using winter 2006 observations from ACE-FTS. In the study by Santee *et al*. (2008), the HCl and ClO measurements from Aura MLS were combined with the $ClONO_2$ and HCl measurements from ACE-FTS and model results from the SLIMCAT chemical transport model to investigate chlorine partitioning during two Arctic and two Antarctic winters. In addition to the ACE-FTS tracer measurements during IPY that were discussed previously (Figure 4), a number of studies are under way using ACE-FTS results from IPY. These include interannual variability in ozone depletion using constituent and tracer measurements from ACE-FTS and MLS (Taylor *et al*., in preparation) and year-to-year differences in energetic particle precipitation enhanced NO_x in the Arctic vortex (Randall *et al*., submitted).

Ground-based Measurements Across the Arctic

The IPY project #196, International Arctic Systems for Observing the Atmosphere (IASOA: **http://www.iasoa.org**) aims to develop a legacy of continuous measurements from existing stations and the newly established intensive Arctic atmospheric observatories, with a focus on measurements of standard meteorology, greenhouse gases, atmospheric radiation, clouds, pollutants, chemistry, aerosols, and surface energy balances. The goal is to develop sufficient understanding to determine relative contributions of natural *versus* anthropogenic forces in shaping the nature of the Arctic atmosphere. Figure 6 shows the distribution of IASOA observatories, along with the six NDACC stations north of 60°N that have FTIR spectrometers.

The facility at Eureka is part of both networks, and comprises a Weather Station, run by Environment Canada, and the Polar Environment Atmospheric Research Laboratory (PEARL), run by the Canadian Network for the Detection of Atmospheric Change (CANDAC: **http://www.candac.org**). PEARL is a refurbishment of an existing laboratory for studying stratospheric ozone, but its mission has been extended to include air quality and climate issues. It is now home to more than 25 instruments that are being used to investigate chemical and physical processes in the atmosphere from the ground to 100 km. These include a range of *in situ* and remote sounding instruments including lidars, radars, spectrometers, radiometers, and samplers.

A new Bruker IFS 125HR FTIR spectrometer was installed at PEARL in July 2006 (Batchelor *et al*., in press). This instrument

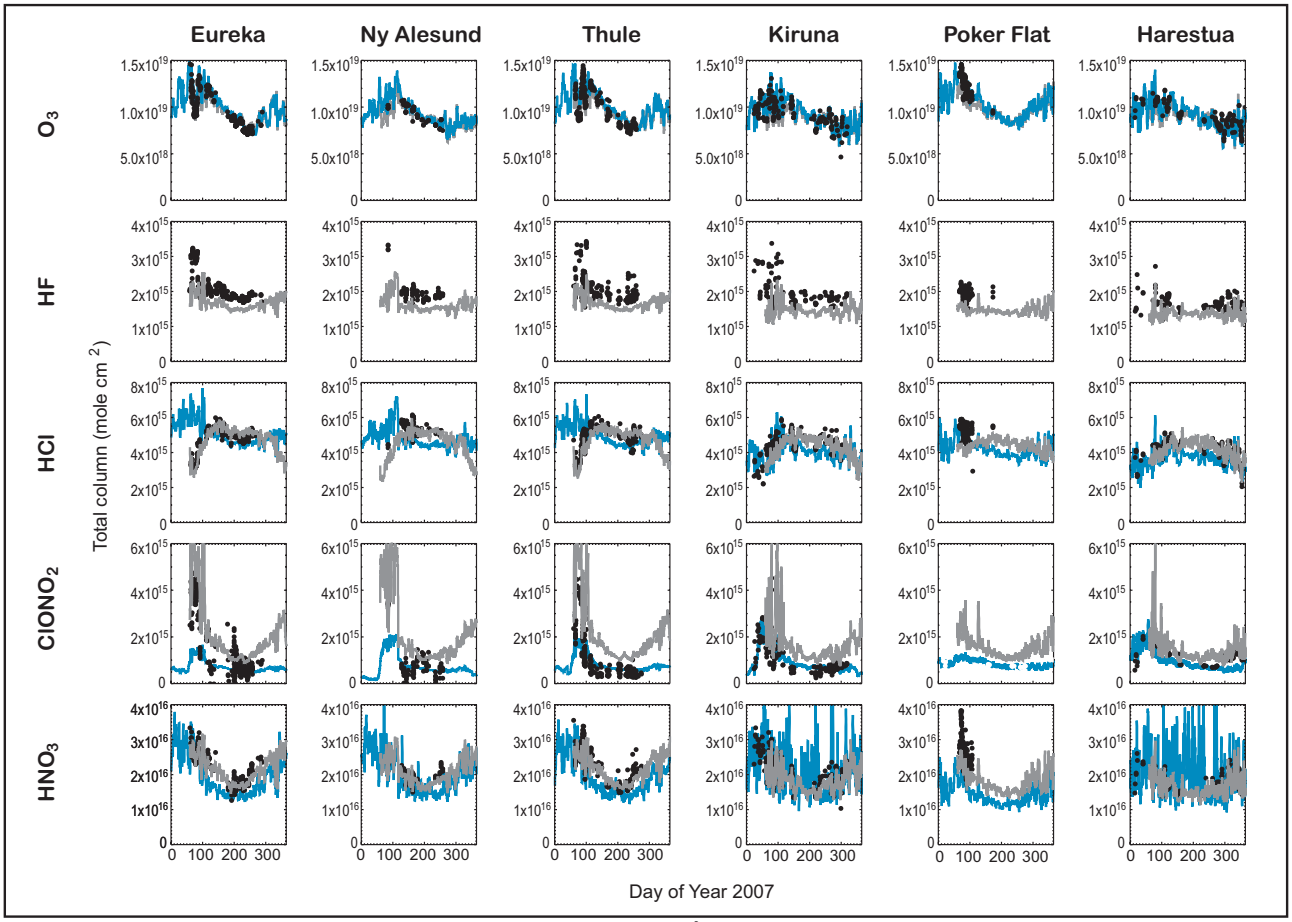

Figure 12. Total columns of ozone, HF, HCl, $ClONO_2$, and HNO_3 at Eureka, Ny Ålesund, Thule, Kiruna, Harestua, and Poker Flat during 2007. FTIR measurements (black circles), GEM-BACH model results (grey lines), and CMAM-DAS model results (blue lines) are shown.

is a very high spectral resolution commercial spectrometer, which is operated semi-autonomously throughout the sunlit parts of the Arctic year. It replaces a Bomem DA8 FTIR that was operated at Eureka by Environment Canada from 1993 to 2008. During the 2007 and 2008 IPY, measurements were made with ground-based FTIR spectrometers at PEARL and at five other NDACC stations around the Arctic. These stations are Eureka, Canada (80°N, 86°W); Ny Ålesund, Spitsbergen (79°N, 12°E); Thule, Greenland (77°N, 69°W); Kiruna, Sweden (68°N, 20°E); Poker Flat, Alaska (65°N, 147°W) and Harestua, Norway (60°N, 11°E).

Figure 12 shows the total columns of five key chemical species involved in stratospheric ozone depletion as measured at each station during 2007: ozone, the fluorine reservoir and tracer HF, chlorine reservoirs HCl and $ClONO_2$, and the nitrogen reservoir HNO_3. In addition, results are displayed from the IPY runs of two global chemistry-climate models[3] with assimilated meteorological variables (winds and temperatures) in the troposphere and stratosphere.

The measurements, in conjunction with dynamical analyses and derived meteorological products, are being utilised to better understand the composition of the Arctic stratosphere during IPY. The high level of variability associated with polar vortex dynamics is clear during the first 100 days of the year, with very different total columns observed at each station depending on whether the measurements are made inside or outside the vortex. Excellent agreement in the ozone columns is seen for both models. However, the CMAM-DAS fails to correctly partition chlorine species within the polar vortex. The high variability observed in the summer-time CMAM-DAS HNO_3 over the European stations Harestua, Kiruna and, to a lesser extent, Ny Ålesund, results from local NO_x emissions in the troposphere that contribute to the HNO_3 total column. This is not observed in the GEM-BACH HNO_3 column as there is no tropospheric chemistry in that model. In general, both models are seen to do a very good job of capturing the polar stratospheric chemistry, with the annual cycle of all of these gases comparing favorably to the FTIR measurements.

While this comparison is preliminary, it illustrates the strength of combining data from different observatories to obtain a more complete picture of the Arctic stratosphere. Polar vortex dynamics tend to dominate the observed columns, and dynamical analyses (not shown) are being used to characterise the underlying vortex conditions at each station. The measurements

[3]These results are available through the Stratospheric Processes and Their Role in Climate (SPARC) Data Center, http://www.sparc.sunysb.edu/): the Canadian Middle Atmosphere Model – Data Assimilation System (CMAM-DAS), and Environment Canada's Global Environmental Multiscale stratospheric model, run with the online BIRA (Belgian Institute for Space Aeronomy) Atmospheric CHemistry package (GEM-BACH)

and the models have a symbiotic relationship: the comparisons enable an assessment of how well the model runs are simulating chemical conditions near the poles (particularly for the meteorological data assimilated runs that have been generated for IPY), while the models, once verified, can contribute to the interpretation of the measurements. We are currently utilising these and other measurements in conjunction with the models and dynamical analyses to better understand conditions in the Arctic stratosphere during IPY.

Quantifying Arctic Chemical Composition in the Future

Continued observations of stratospheric composition are essential for ascertaining that the ozone layer is 'recovering' as expected, and for quantifying its progress and the impact of climate change on this recovery. In addition to observing the decrease in stratospheric halogens, global vertically-resolved composition profile observations are critical to quantifying changes in stratospheric dynamics and meteorology that can strongly modulate ozone layer recovery. Quantification of chemical ozone loss in the Antarctic and Arctic stratosphere requires the separation of complex chemical and dynamical influences on ozone, for which continued daily global vertically-resolved composition observations, including during polar night, are essential.

Our understanding of critical chemical, dynamical, and radiative processes in the stratosphere has advanced dramatically over the last two decades, thanks in large part to the wealth of composition observations from satellite, airborne, and ground-based instruments. However, the diversity and frequency of such observations is waning. Aircraft and balloon flights are less frequent than in previous years, and resources for ground-based observations are diminishing. The Arctic is a remote and difficult environment: maintaining stations and data records is an ongoing challenge. It is critical that we continue to acquire the long-term measurements that are the strength of ground-based instruments.

All of the satellites making stratospheric composition profile measurements are currently, or will shortly be, operating in "extended mission" (*i.e.*, beyond their design lifetimes). Plans for successor missions are sketchy at best, with the only confirmed stratospheric observations being ozone profiles measured by ultraviolet limb scatter (thus limited to daylight) from the OMPS (Ozone Mapping and Profiler Suite) instrument to launch on the NPOESS Preparatory Project (NPP) spacecraft no earlier than Spring 2011. The Japanese SMILES (Superconducting Submilimeter-wave Limb Emission Sounder) instrument to be installed on the International Space Station (ISS) in 2009 will make high precision microwave limb composition profile measurements in the stratosphere and mesosphere. However, observations are restricted to 38°S to 65°N, and the nominal "prime mission" duration is only one year. A significant gap in stratospheric observations is anticipated between NASA's Aura satellite and the expected successor Global Atmospheric Composition Mission (GACM). A similar gap between ESA's Envisat and Sentinel 5 missions is highly likely. The long and valuable record of high precision, high vertical resolution solar occultation observations from the Polar Ozone and Aerosol Measurement (POAM) and Stratospheric Aerosol and Gas Experiment (SAGE) series of instruments, and from the Halogen Occultation Experiment (HALOE) on UARS, is currently being extended only by the Canadian Atmospheric Chemistry Experiment Fourier Transform Spectrometer (ACE-FTS), and there are no confirmed plans for future occultation measurements.

Summary

In this article we have presented an overview of the Arctic wintertime stratospheric circulation and chemistry that has been revealed by ground-based lidar, FTIR spectrometer and satellite measurements that have become available during the IPY period. Of necessity this overview is broad and not detailed in its perspective. However, as noted in the references, a substantial amount of detailed work has already been published in peer reviewed journal articles and more will appear in forthcoming papers.

Much progress has been made toward preparing the comprehensive picture of the structure and evolution of the Arctic polar vortex that was originally envisaged as a major goal of SPARC-IPY and its linked IPY activities. It is clear that such a goal would have much less achievable in the absence of the coincidence of a critical combination of ground-based and satellite measurement systems and observations.

An extended record of stratospheric composition observations is critical for placing our understanding of the stratosphere and its future evolution on a sound scientific footing. We have drawn attention to the looming and profound gap in stratospheric composition observations from satellites. This is an issue of particular concern to the SPARC community.

Acknowledgements

The authors are grateful to many colleagues for encouragement, helpful comments and assistance during the course of IPY.

Work at the Jet Propulsion Laboratory, California Institute of Technology, was performed under contract with the National Aeronautic and Space Administration. The Atmospheric Chemistry Experiment (ACE), also known as SCISAT, is a Canadian-led mission mainly supported by the Canadian Space Agency and the Natural Sciences and Engineering Research Council of Canada.

The authors gratefully acknowledge the contributions of G. Baumgarten, J. Fiedler, B.J. Firanski, M. Gerding, J. Höffner, J.M. Livingston, F.-J. Lübken, K. Mizutani, R.J. Sica, K.B. Strawbridge, and B. Thurairajah in acquiring, analysing and providing the Rayleigh lidar data; the US National Science Foundation Arctic Observing Network for the IPY Rayleigh lidar network; the CANDAC, Environment Canada, the National Science Foundation, ALOMAR, Norway and the Leibniz-Institute of Atmospheric Physics, Germany, for lidar operations at PEARL, Kangerlussuaq, Andoya and Kühlungsborn; the Atlantic Innovation Fund/Nova Scotia Research Innovation Trust, Canadian Foundation for Climate and Atmospheric Sciences (CFCAS), Canadian Foundation for Innovation, Canadian Space Agency, Environment Canada, Government of Canada International Polar Year funding, Indian and Northern Affairs Canada, Natural Sciences and Engineering Research Council, Ontario Innovation Trust, Polar Continental Shelf Program and the Ontario Research Fund for funding CANDAC and PEARL; the United Nations Environment Programme (UNEP), the International Ozone Commission (IOC) of the International Association of Meteorolo-

gy and Atmospheric Physics and the World Meteorological Organization (WMO) as a major contributor of WMO's Global Atmosphere Watch (GAW) for endorsing NDACC; the NDACC FTIR community for providing the FTIR data, in particular R. Batchelor, T. Blumenstock, M. Coffey, J. Hannigan, F. Hase, A. Kagawa, Y. Kasai, J. Klyft, R. Lindenmaier, J. Mellqvist, J. Notholt, M. Palm, A. Strandberg, and K. Strong for the FTIR data from Eureka, Ny Ålesund, Thule, Kiruna, Poker Flat, and Harestua; the National Aeronautics and Space Administration and the National Science Foundation, the sponsor of the National Center for Atmospheric Research, for the measurement program at Thule; the Environment Canada-Belgian collaboration for GEM-BACH analyses; and CFCAS and the Canadian Space Agency for CMAM-DAS analyses which were produced by a university-Environment Canada collaboration.

IASOA is led by T. Uttal (NOAA) and J.R. Drummond (Dalhousie University/University of Toronto), who is also CANDAC/PEARL Principal Investigator.

References

Andrews, D.G., *et al*., *Middle Atmosphere Dynamics*, Academic Press, San Diego, California, 1987.

Batchelor, R.L, K. Strong, *et al*., A new Bruker IFS 125HR FTIR spectrometer for the Polar Environment Atmospheric Research Laboratory at Eureka, Canada - Measurements and comparison with the existing Bomem DA8 spectrometer, *J. Atmos. Oceanic Technol*., doi: 10.1175/2009JTECHA1215.1, in press.

Bernath, B.F., *et al*., Atmospheric Chemistry Experiment (ACE): mission overview, *Geophys. Res. Lett*., **32**, L15S01, doi:10.1029/2005GL022386, 2005.

Charlton, A.J., and L.M. Polvani, A new look at stratospheric sudden warmings. Part I: Climatology and modeling benchmarks, *J. Clim.*, **20**, 449–469, 2007.

Dufour, G., *et al*., Partitioning between the inorganic chlorine reservoirs HCl and ClONO2 during the Arctic winter 2005 from the ACE-FTS, *Atmos. Chem. Phys*., **6**, 2355-2366, 2006.

Dunkerton, T.J., and N. Butchart, Propagation and selective transmission in internal gravity waves in a sudden warming, *J. Atmos. Sci*., **41**, 1443-1460, 1984.

Harvey V.L., *et al*., A climatology of stratospheric polar vortices and anticyclones, *J. Geophys. Res*., **107**, 4442, doi:10.1029/2001JD001471, 2002.

Hauchecorne, A., *et al*., Large increase of NO_2 in the north polar mesosphere in Janaury-February 2004: Evidence of a dynamical origin from GOMOS/ENVISAT and SABER/TIMED data, *Geophys. Res. Lett*., **34**, L03810, doi:10.1029/2006GL027628, 2007.

Hoffmann, P., W. Singer, D. Keuer, W. K. Hocking, M. Kunze, and Y. Murayama, Latitudinal and longitudinal variability of mesospheric winds and temperatures during stratospheric warming events, *J. Atmos. Sol. Terr. Phys*., **69**, 2355– 2366, 2007.

Jin, J.J., *et al*., Denitrification in the Arctic Winter 2004/2005: Observations from ACE-FTS, *Geophys. Res. Lett.*, **33**, L19814, doi:10.1029/2006GL027687, 2006.

Manney, G.L., *et al*., Aura Microwave Limb Sounder Observations of Dynamics and Transport During the Record-breaking 2009 Arctic Stratospheric Major Warming, *Geophys. Res. Lett*., doi: 10.1029/2009GL038586, in press.

Manney, G.L., *et al*., Satellite observations and modelling of transport in the upper troposphere through the lower mesosphere during the 2006 major stratospheric sudden warming, atmos. *Chem. Phys. Disc*., **9**, 9693-9745, 2009.

Manney, G.L., *et al*., The evolution of the stratopause during the 2006 major warming: Satellite Data and Assimilated Meteorological Analyses, J. *Geophys. Res.*, **113**, D11115, doi:10.1029/2007JD009097, 2008.

Manney, G.L., *et al*., The high arctic in extreme winters: Vortex, temperature, and MLS and ACE-FTS trace gas evolution, *Atmos. Chem. Phys*., **8**, 505-522, 2008.

Manney, G.L., *et al*., EOS MLS observations of ozone loss in the 2004-2005 Arctic winter, *Geophys. Res. Lett*., **33**, L04802, doi:10.1029/2005GL024494, 2006.

Manney, G.L., *et al*., The remarkable 2003-2004 winter and other recent warm winters in the Arctic stratosphere since the late 1990s, *J. Geophys. Res*., **110**, D04107, doi:10.1029/2004JD005367, 2005.

Manney, G. L., *et al*., On the motion of air through the stratospheric polar vortex, *J. Atmos. Sci*., **51**, 2973-2994, 1994.

Montzka, S.A., *et al*., A decline in tropospheric organic bromine, *Geophys. Res. Lett*., **30**, 1826, 2003.

Randall, C.E., *et al*., Enhanced NO_x in 2006 linked to strong upper stratospheric Arctic vortex, *Geophys. Res. Lett*., **33**, L18811, doi:10.1029/2006GL027160, 2006.

Randall, C.E., *et al*., NO_x descent in the Arctic middle atmosphere in early 2009, *Geophys. Res. Lett*., submitted.

Rösevall, J.D., *et al*., A study of ozone depletion in the 2004/2005 Arctic winter based on data from Odin/SMR and Aura/MLS, J. *Geophys. Res*., **113**, D13301, doi:10.1029/2007JD009560, 2008.

Sica, R.J., *et al*., Validation of the Atmospheric Chemistry Experiment (ACE) version 2.2 temperature using ground-based and space-borne measurements, *Atmos. Chem. Phys*., **8**, 35-62, 2008.

Santee, M.L., *et al*., A study of stratospheric chlorine partitioning based on new satellite measurements and modeling, *J. Geophys. Res*., **113**, D12307, doi:10.1029/2007JD009057, 2008.

Schoeberl, M.R., *et al*., Chemical observations of a polar vortex intrusion, *J. Geophys. Res*., **111**, D20306, doi:10.1029/2006JD007134, 2006.

Singleton, C.S., *et al*., Quantifying Arctic ozone loss during the 2004-2005 winter using satellite observations and a chemical transport model, *J. Geophys. Res*., **112**, D07304, doi:10.1029/2006JD007463, 2007.

Siskind, D.E., *et al*., On recent interannual variability of the Arctic winter mesosphere: Implications for tracer descent, *Geophys. Res. Lett*., **34**, L09806, doi:0.029/2007GL029293, 2007.

Taylor, J.R., *et al*., Observed inter-annual variability of O_3 and related constituents in the Arctic lower stratosphere, in preparation.

Thurairajah, B., *et al*., Multi-Year Temperature Measurements of the Middle Atmosphere at Chatanika, Alaska (65°N, 147°W), *Earth Planets and Space*, in press.

Waters, J. W., *et al*., The Earth Observing System Microwave Limb Sounder (EOS MLS) on the Aura satellite, *IEEE Trans. Geosci. Remote Sens*., **44**, 1075-1092, 2006.

Wilson, R., *et al*., Gravity waves in the middle atmosphere observed by Rayleigh lidar 2. Climatology, *J. Geophys. Res.*, **96**, 5169-5183, 1991.

WMO, World Meteorological Organization/United Nations Environment Programme (WMO/UNEP), Scientific Assessment of Ozone Depletion: 2006, Rep. 50, 572 pp., Geneva, Switzerland, 2007.